Clin Transl Oncol (2015) 17:795–802
DOI 10.1007/s12094-015-1307-x

RESEARCH ARTICLE

Sodium/iodide symporter gene transfection increases radionuclide uptake in human cisplatin-resistant lung cancer cells

W. Chai[1,2] · X. Yin[1] · L. Ren[1] · M. Cai[1] · T. Long[1] · M. Zhou[1] · Y. Tang[1] · N. Yang[1] · S. Hu[1]

Received: 29 June 2014 / Accepted: 22 May 2015 / Published online: 27 June 2015

Abstract The sodium/iodide symporter (NIS) is involved in iodide uptake and has been used for the diagnosis and treatment of thyroid cancer. Transfection of the NIS gene in A549 human lung cancer cells can induce radioactive iodine (^{131}I) and radioactive technetium (^{99m}Tc) uptake. The aim of the present study was to assess the role of NIS in ^{99m}Tc and ^{131}I uptake by the A549/DDP human cisplatin-resistant lung cancer cell line. To do so, recombinant adenovirus, adenovirus-enhanced green fluorescent protein-human NIS (Ad-eGFP-hNIS) and Ad-eGFP-rat NIS (Ad-eGFP-rNIS) vectors were established. These vectors were transfected into A549/DDP cells and xenograft tumors in nude mice. Assessment of ^{99m}Tc and ^{131}I uptake was performed. Results showed that the transfection efficiency of Ad-eGFP-hNIS and Ad-eGFP-rNIS in A549/DDP cells was at least 90 % in all experiments, and that the uptake ability of ^{99m}Tc and ^{131}I was highly enhanced (14–18 folds for ^{99m}Tc, and 12–16 folds for ^{131}I). However, the radionuclide concentration in transfected NIS genes' A549/DDP cells reached a plateau within 30–60 min, indicating that NIS transport led rapidly to ^{99m}Tc and ^{131}I saturation in cells. In xenograft tumor models, uptake of $^{99m}TcO_4^-$ was obviously higher in the hNIS and rNIS groups compared with controls. In conclusion, these results support the hypothesis that A549/DDP cells can effectively uptake ^{99m}Tc and ^{131}I when transfected with the hNIS and rNIS gene. The rNIS or hNIS gene could be used as an effective method for the effective delivery of radioactive products to specific tissues for imagery and/or treatment.

Keywords Sodium/iodide symporter gene · Transfection · Radionuclide · Lung cancer

Introduction

Lung cancer, originating from epithelial cells of the bronchial mucosa and lung tissue, has become one of the most common cancers and one of the most difficult tumors to treat, with 1.6 million new cases and 1.38 million deaths in 2008 in the world [1]. Although lung cancer can be treated by surgery, radiation, and drugs, the 5-year survival rate remains under 15 %, mainly because of the lack of effective early diagnosis methods and of the occurrence of inherent and acquired resistance to drugs [2, 3]. Thus, effective methods for the early diagnosis and to overcome chemoresistance of lung cancer may help to reduce lung cancer incidence and mortality. The present study presents a promising potential of NIS-mediated radionuclide imaging and therapy for treatment-resistant lung cancer.

In recent years, targeted gene cancer therapy received much attention. Compared with the traditional surgery, radiation and chemotherapy approaches, gene therapy is one of the most promising therapeutic approaches for cancer due to its high targeting potential, its lack of side effects and its lack of damage to normal cells [4–6]. With the development of molecular imaging, noninvasive molecular imaging using reporter genes is a relatively

Electronic supplementary material The online version of this article (doi:10.1007/s12094-015-1307-x) contains supplementary material, which is available to authorized users.

✉ S. Hu
18163637568@126.com

[1] Department of Nuclear Medicine, Xiangya Hospital, Central South University, No. 87 Xiangya Road, Changsha 410008, Hunan, China

[2] Department of Nuclear Medicine, Hu Nan Tumor Hospital, Changsha 410008, China

recent field of research that shows great promises for cancer diagnosis and therapy [7, 8]. However, a number of issues remain to be addressed before gene therapy can be used in clinical settings.

Historically, thyroid imagery using ^{99m}Tc or ^{131}I has played a key role in diagnosis and treatment of thyroid cancer [9]. The sodium/iodide symporter (NIS) is a transmembrane glycoprotein in thyroid follicular cells at the basolateral pole and mediates the active iodide uptake in the thyroid gland [10]. NIS expression can be easily imaged using simple radiotracers, such as ^{99m}Tc and/or ^{131}I. Previous studies showed that rat NIS (rNIS) and human NIS (hNIS) could be used as reporter genes to invasively monitor rat bone marrow mesenchymal stem cells (rBMSCs) transplanted into infarcted rat myocardium [11]. In addition, NIS has also been used in a therapeutic gene approach to treat cancers through its ability to concentrate therapeutic doses of radionuclides in target cells, such as lung cancer, colon cancer and hepatocellular cancer [12–15]. However, there is a lack of data about the use of NIS as an imaging reporter gene in chemoresistant lung cancer cells.

Therefore, the aim of the present study was to assess the transfection efficiency of hNIS and rNIS in A549/DDP cisplatin-resistant lung cancer cells, to assess the ability of these transfected cells to uptake ^{99m}Tc and/or ^{131}I, and to perform imagery of xenograft tumor models generated from these cells. We hypothesized that NIS can be efficiently used to concentrate radionuclides in chemoresistant lung cancer cells, allowing to image the cells. Results from the present study could eventually lead to new imaging and treatment approaches in chemoresistant lung cancers using a gene therapy approach.

Materials and methods

Cell culture

The human cisplatin-resistant lung cancer A549/DDP and A549 cell lines (Xiangya School of Medicine Type Culture Collection, China) were cultured in DMEM (Hyclone, Thermo Fisher Scientific, Waltham, MA, USA) with 10 % heat-inactivated fetal bovine serum (FBS) at 37 °C, in 5 % CO_2. Cells were passaged when they grew to 70–80 % confluence.

Adenoviral vector construction

The hNIS and rNIS plasmids were provided by Prof. Carrasco (Albert Einstein Medical School Molecular Pharmacology Laboratory, Yeshiva University, New York, NY, USA). The plasmid was excised by *Eco*RI/*Hin*dIII digestion and connected with pShuttle-eGFP-CMV (-)TEMP, and then cloned into a pAdxsi vector. Both Ad-eGFP-hNIS and Ad-eGFP-rNIS were transfected into HEK293 cells for amplification. The viral particles were collected and the titer was determined following a previously published method [11].

Toxicity of Ad-eGFP-hNIS and Ad-eGFP-rNIS in cells

The A549/DDP cells were seeded in a 96-well plate for 24 h. Solutions containing Ad-eGFP-hNIS and Ad-eGFP-rNIS with different multiplicities of infection (MOI) (0, 100, 200, 400, 800, 1000, 1600, 2000, and 3000) were then added to the cells and incubated; viral solutions were replaced with fresh DMEM after 4 h. Forty-eight hours later, 3-(4,5-dimethyl-2-thiazolyl)-2,5-diphenyl-2-H-tetrazolium bromide (MTT) (20μL/well, 10 mg/mL) was added to the cells. The supernatant was removed and changed with dimethyl sulfoxide (DMSO, 150 μL/well), and the cells were further incubated for 4 h. Optical density (OD) values were measured by spectrophotometer at 490 nm.

Adenoviral infection of cells

To determine the optimal MOI for transfection, cells were plated into six-well plates (5×10^5 cells/well) to reach 70–80 % confluence before adding Ad-eGFP-hNIS or Ad-eGFP-rNIS solutions with different MOI (0, 800, 1000, 1600, and 2000) to A549/DDP and A549 cells. After 4 h of incubation, the medium was changed with fresh DMEM. Twenty-four hours later, the cells were observed under a fluorescence microscope and were detected by flow cytometry.

Reverse transcription PCR (RT-PCR) for NIS gene expression

After transfecting the NIS gene into A549/DDP cells using the optimal MOI for 48 h, total RNA was isolated using Trizol (Invitrogen Inc., Carlsbad, CA, USA), according to the manufacturer's instructions. RNA concentration and purity were assessed with a spectrophotometer at 260 and 280 nm. RNA was reverse transcribed into cDNA using a Primescript^{TM} RT reagent kit (Invitrogen Inc., Carlsbad, CA, USA), according to the manufacturer's instructions. Primers were: β-actin: forward, 5′-TCCTTCCTGGGCA TGGAGTC-3′ and reverse, 5′-GTAACGCAACTAAGTC ATAGTC-3′; hNIS: forward, 5′-GTCGTGGTGATG CTA AGTGGC-3′ and reverse, 5′-ATTGATGCTGGTGGATG CTGT-3′); and rNIS: forward, 5′-AAGTTCCTGTGGATG TGCG-3′ and reverse, 5′-TCACACCGTACATGGAGAG C-3′. β-Actin was used as an internal control to evaluate the relative expressions of hNIS and rNIS. NIS PCR

conditions were: denaturation at 94 °C for 2 min, followed by 30 cycles of 94 °C for 30 s, 61 °C for 30 s (β-actin: 50 °C for 30 s), 72 °C for 30 s, then by a 2-min elongation at 72 °C. PCR products were analyzed by 1.0 % agarose gel electrophoresis. Gels were stained with ethidium bromide, photographed and scanned using the Band Leader 3.0 software for gray scale semi-quantitative analysis.

Radionuclide uptake studies

The ability of the cells to concentrate ^{99m}Tc or ^{131}I was determined as previously described by Jeon et al. [14]. The cells were seeded in 24-well plates (1×10^5 cells/well) and transfected using Ad-eGFP-hNIS or Ad-eGFP-rNIS solutions with different MOI (0, 400, 800, 1000, 1600, and 2000) for 48 h. ^{99m}Tc-pertechnetate solution (Atom Gaoke, Beijing, China) (740 MBq/mL, 10 μL/well) or ^{131}I solution (Atom Gaoke, Beijing, China) (3.7 MBq/mL, 50 μL/well) was added and the cells were incubated for 1 h at 37 °C. Cells were washed twice with ice-cold phosphate-buffered saline (PBS) and dissolved in 0.1 % NaOH. Cell lysates were then collected and the radioactivity accumulated in the cells was measured using a gamma counter (Zonkia Scientific Instruments Co., LTD, Anhui, China). For the blocking experiment, transfected A549/DDP cells were incubated with $KClO_4$ (10 mmol/L, 20 μL/well), ^{99m}Tc or ^{131}I. After cell lysis performed as above, cell uptake of ^{99m}Tc or ^{131}I was measured by a gamma counter.

To determine the radionuclide uptake in relation to incubation time, A549/DDP cells transfected or not with Ad-eGFP-hNIS or Ad-eGFP-rNIS solution were cultured with 7.4 MBq^{99m}Tc or 175 KBq^{131}I for 5, l0, 20, 30, 60, 90, and 120 min. Radionuclide absorption was determined as above.

Cells were plated, infected and incubated as described for the radionuclide efflux studies. After incubated for 1 h with medium containing 7.4 MBq ^{99m}Tc or 175 kBq ^{131}I, when the intracellular nuclide reached a steady level, cells were washed twice and lysed immediately. Fresh DMEM medium was added to the remaining wells. The cells were again incubated for 5, 10, 20 or 30 min and lysed as described.

Adenoviral infection of tumor xenografts

Male nude mice (4–6 weeks of age) were purchased from Slac Laboratory Animal (Hu Nan, China) and were housed in our facility under constant temperature (25–27 °C), constant humidity (25–50 %) and specific pathogen-free conditions. A week after adaptation feeding, tumor models were induced by subcutaneous injection of 200 μL of sterile PBS containing 5×10^6 A549/DDP cells in the right armpit.

Mice with tumors $\geq$150 mm^3 received intratumoral injections of 5×10^9 plaque-forming units of recombinant Ad-eGFP-hNIS or Ad-eGFP-rNIS solution or sterile PBS in a total volume of 100 μL of PBS using tuberculin syringes with 27-gauge needles. The needle was moved to various sites within the tumor during injection to maximize the area of virus exposure.

In vivo tumor imaging

Three days after injection of virus into the A549/DDP tumors, mice were given a tail injection of 37 MBq of $^{99m}TCO_4^-$. Static SPECT images were acquired after 10 min using a gamma camera (GE Healthcare, Waukesha, WI, USA) with a low-energy, high-resolution collimator.

Biodistribution

Mice were sacrificed at the end of SPECT scan (90-min time point). Blood, heart, liver, spleen, lung, kidneys, thyroid, stomach, intestine, muscle, bone and tumor were harvested and weighed. Radioactivity was measured by a gamma counter and the corresponding CPM count/mg tissue was calculated.

Statistical analysis

Statistical analysis was performed using SPSS 17.0 (IBM, Armonk, NY, USA). Data are expressed as mean ± standard deviation (SD). ANOVA was used to assess the statistical differences among groups. A P value <0.05 was considered significant.

Results

Toxicity of Ad-eGFP-hNIS and Ad-eGFP-rNIS in A549/DDP cells

The toxic effect of different titers of Ad-eGFP-hNIS and Ad-eGFP-rNIS inA549/DDP cells is shown in Table 1. When the MOI were less than 3000, cell viability was virtually unaffected in the hNIS and rNIS groups, as determined by MTT assays.

Transfection efficiency of Ad-eGFP-hNIS and Ad-eGFP-rNIS

In the present study, 800 MOI were defined as the optimal MOI instead the generally used 200. The transfection efficiencies of Ad-eGFP-rNIS in A549/DDP cells were 91.0 and 85.1 % using 800 and 200 MOI, respectively. The uptake ability of ^{99m}Tc and ^{131}I was highly enhanced in the transfected A549/DDP cells using 800 MOI, while the uptake ability was lower in A549/DDP cells transfected

Table 1 Toxicity of Ad-eGFP-hNIS and Ad-eGFP-rNIS to A549/DDP cells

MOI	0	100	200	400	800	1000	1600	2000	3000
Ad-eGFP-hNIS	0.95 ± 0.07	1.02 ± 0.05	0.98 ± 0.03	1.02 ± 0.08	1.00 ± 0.04	0.98 ± 0.06	0.86 ± 0.07	0.88 ± 0.01	0.86 ± 0.01
Ad-eGFP-rNIS	1.00 ± 0.07	0.98 ± 0.09	0.95 ± 0.02	0.96 ± 0.04	0.94 ± 0.06	0.95 ± 0.12	0.90 ± 0.04	0.91 ± 0.07	0.88 ± 0.04

MOI multiplicities of infection, *Ad-eGFP-hNIS* adenovirus-enhanced green fluorescent protein-hNIS, *Ad-eGFP-rNIS* adenovirus-enhanced green fluorescent protein-rNIS

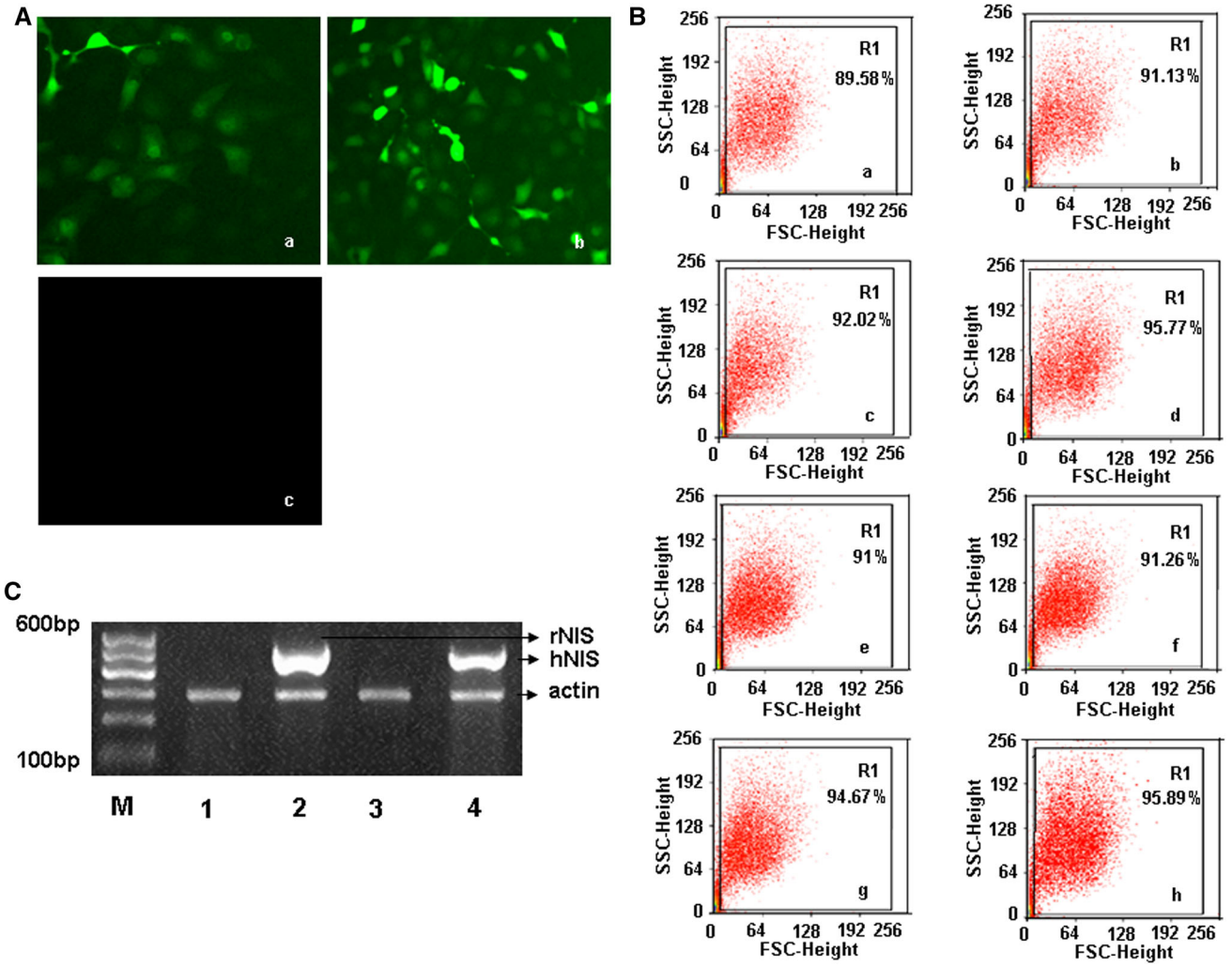

Fig. 1 Transfection efficiency of Ad-eGFP-hNIS and Ad-eGFP-rNIS. **A** Expression of the fluorescent reporter protein. Cells were incubated with Ad-eGFP-hNIS (*a*) orAd-eGFP-rNIS (*b*) for 48 h, at a MOI of 800, and visualized using a fluorescence microscope (×200). Untransfected cells did not express the reporter protein (*c*). **B** Transfection efficiency of adenoviral vectors in A549/DDP cells by flow cytometry. Both hNIS and rNIS genes were transfected into A549/DDP cells. Transfection efficiency of hNIS with different MOI. *a–d* Transfection efficiency of hNIS with MOI 800, 1000, 1600, 2000. *e–h* Transfection efficiency of rNIS with MOI 800, 1000, 1600, 2000. **C** NIS gene expression in A549/DDP cells. RT-PCR analysis of hNIS and rNIS in A549/DDP cells. β-actin was used as control. *1* Ad-eGFP-rNIS control group; *2* Ad-eGFP-rNIS-transfected group; *3* Ad-eGFP-hNIS control group; *4* Ad-eGFP-hNIS-transfected group; *M* standard reference

using 200 MOI. A549/DDP cells were resistant to cisplatin while A549 cells were sensitive to cisplatin (Supplemental Figure 1). There was no obvious difference between A549/DDP and A549 cells in transfection efficiency with the same MOI when using MOI from 200 to 800, although the green fluorescence intensity in transfected A549/DDP cells was significantly lower than that in transfected A549 cells (Supplemental Figures 2, 3). The reason might be that the

transfected A549/DDP cells inhibited the expression of eGFP and NIS proteins to a certain degree compared with transfected A549 cells.

The transfection efficiency of Ad-eGFP-hNIS and Ad-eGFP-rNIS in A549/DDP cells was gradually increased with increasing titer, as determined by flow cytometry and confirmed by visualizing eGFP-positive cells under the microscope (Fig. 1). The NIS-transfected cells were visible using green fluorescence compared with untransfected cells (Fig. 1A). The transfection efficiency of Ad-eGFP-hNIS was 89.58, 91.13, 92.02, and 95.77 % when the MOI were 800, 1000, 1600 and 2000, respectively. The transfection efficiency of Ad-eGFP-rNIS was 91.0, 91.26, 94.67, and 95.89 % when the MOI were 800, 1000, 1600 and 2000, respectively (Fig. 1B). There was no significant difference in the transfection efficiency of Ad-eGFP-hNIS and Ad-eGFP-rNIS in A549/DDP cells after 48 h. Given that a MOI of less than 3000 induced no toxicity to the cells, 800 was defined as the optimal MOI.

hNIS and rNIS expression levels in transfected A549/DDP cells were investigated by RT-PCR analysis. hNIS and rNIS expression in transfected A549/DDP cells was much higher than in untransfected cells (Fig. 1C).

Radionuclide uptake experiments

To measure ^{99m}Tc and ^{131}I cells uptake, transfected and untransfected A549/DDP cells were incubated with ^{99m}Tc or ^{131}I for 1 h, and radioactivity in the cells was measured by a gamma counter. Ad-eGFP-hNIS cells had a 14-fold higher uptake of ^{99m}Tc compared with untransfected cells, and Ad-eGFP-rNIS cells showed >18-fold higher levels. Meanwhile, Ad-eGFP-hNIS and Ad-eGFP-rNIS cells had a 12- and 16-fold higher ^{131}I uptake, respectively, than wild-type cells (Fig. 2A). The uptake of ^{99m}Tc and ^{131}I can both be completely blocked by adding $KClO_4$ (Fig. 2B).

The uptake of ^{99m}Tc and ^{131}I in transfected cells rapidly reached a plateau at 30–60 min, as shown in Fig. 2C. There was also a significant difference in the uptake between cells transfected by Ad-eGFP-hNIS and Ad-eGFP-rNIS ($P = 0.008$).

To determine the ^{99m}Tc and ^{131}I efflux, cells were allowed to uptake radionuclide for 1 h, time at which a steady-state level of accumulation was achieved. As shown in Fig. 2D, the cellular radioactivity in transfected cells was continuously released, resulting in an effective half-life of approximately 5 min and 80 % efflux after 30 min.

In vivo imaging and biodistribution of $^{99m}TcO_4^-$ in tumor-bearing rats

After establishing the xenograft tumor models, SPECT was performed on all rats after intravenous injection of $^{99m}TcO_4^-$. The 10-min static SPECT showed that the NIS-expressing tumor tissue accumulated $^{99m}TcO_4^-$ rapidly and significantly, leading to scintigraphic visualization, whereas the control tumor was not visualized (Fig. 3A). Normal NIS-expressing tissues, including the thyroid gland and stomach, were also clearly visible. The transfected tumor imaging was more and more obvious with elapsing time (Fig. 3A).

The biodistribution data are summarized in Fig. 3B after injection of $^{99m}TcO_4^-$ into the lateral tail vein. The NIS-expressing tumors exhibited an increased uptake of $^{99m}TcO_4^-$ compared with untransfected tumors. Uptake mediated by hNIS and rNIS was higher than in the untransfected tumor tissue. Except for the thyroid gland and stomach, there was no significant difference among other tissues compared with the control group.

Discussion

NIS allows the treatment of differentiated thyroid cancer using radioiodine [16, 17]. Gene therapy is a promising approach in lung cancer for which traditional treatment approaches failed [4–6]. NIS has been used in a therapeutic gene approach to treat cancers through its ability to concentrate therapeutic doses of radionuclide in target cells [12–15]. However, there is a lack of data about the use of NIS as an imaging reporter gene in chemoresistant lung cancer cells. Therefore, the aim of the present study was to assess the transfection efficiency of hNIS and rNIS in A549/DDP cisplatin-resistant lung cancer cells, to assess the ability of these transfected cells to uptake ^{99m}Tc and/or ^{131}I, and to perform imagery of xenograft tumor models generated from these cells.

However, the radionuclide concentration in transfected A549/DDP cells reached a plateau within 30–60 min, indicating that NIS transport led rapidly to ^{99m}Tc and ^{131}I saturation in cells. In xenograft tumor models, uptake of $^{99m}TcO_4^-$ was obviously high in the hNIS and rNIS groups compared with controls.

NIS is an intrinsic membrane glycoprotein and plays an important role for the biosynthesis of thyroid hormones as it mediates the active transport of iodide [10]. The cloning of the rat and human NIS genes in 1996 paved the way to treat non-thyroid tumors and thyroid tumors that could not uptake iodide [18, 19]. However, the main problem was to induce tumor cells to uptake and express the NIS gene. Presently, a number of different viral vectors were used in clinical trials because of their high efficiency, simple preparation, high recombinant virus titer and large heterologous gene segments [20]. A previous study showed the feasibility of using baculovirus to transfect NIS into A549 cells [21]. Klutz studied a NIS-delivering synthetic

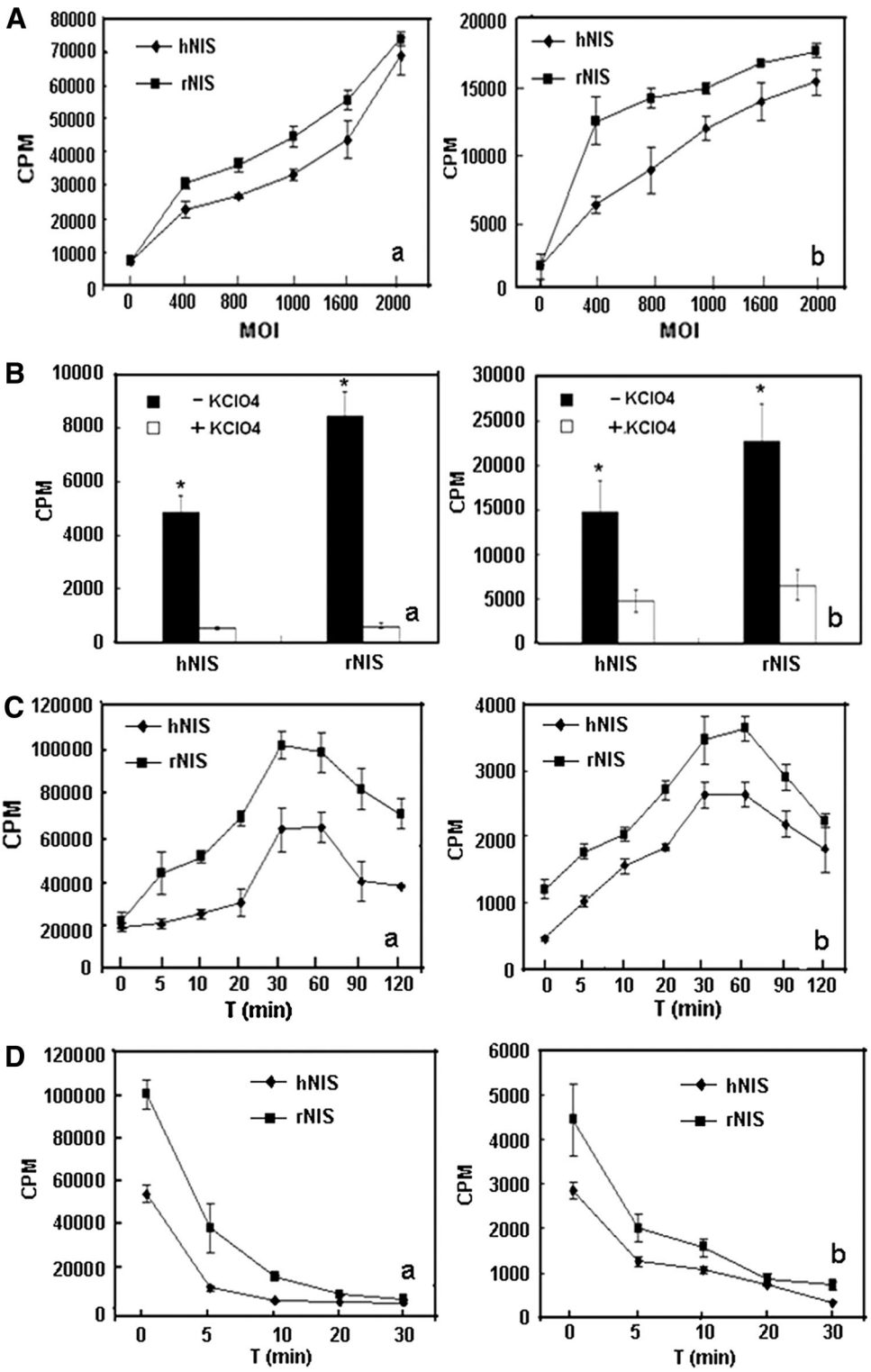

Fig. 2 Radionuclide uptake studies. **A** Radionuclide uptake experiments. After incubation of ^{99m}Tc (*a*) or ^{131}I (*b*) for 1 h, uptake by the transfected cells was significantly increased. **B** Radionuclide uptake inhibition experiments. The uptake of ^{99m}Tc (*a*) and ^{131}I (*b*) could both be completely blocked by $KClO_4$ in hNIS- or rNIS-transfected cells. **C** Dynamic uptake experiments. The uptake of ^{99m}Tc (*a*) and ^{131}I (*b*) in transfected cells was rapid, reaching a plateau at 30–60 min. **D** Radionuclide efflux experiments. The ^{99m}Tc (*a*) and ^{131}I (*b*) were secreted quickly from the transfected cells

polymeric vector in neuroblastomas [22]. In this present study, the NIS gene was transfected into A549/DDP cells by adenovirus vectors. The expression levels of hNIS and rNIS were higher in transfected A549/DDP cells compared with untransfected cells. Meanwhile, the experiments also showed that the transfection efficiency was gradually enhanced with the progressive increase in the titer.

In the present study, A549/DDP cells transfected with Ad-eGFP-hNIS and Ad-eGFP-rNIS could effectively uptake radionuclide, which was inhibited by $KClO_4$.

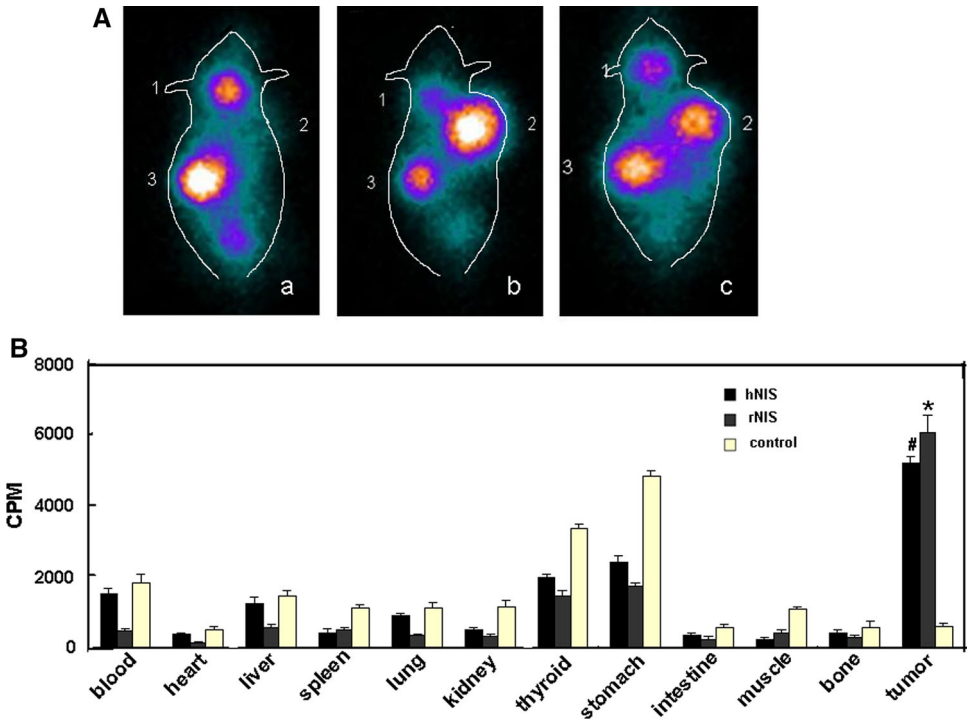

Fig. 3 In vivo imaging and biodistribution of $^{99m}TcO_4^-$ in tumor-bearing rats. **A** Whole-body scintigraphic images of bearing-tumor mice 10 min after tail injection of ^{99m}Tc-pertechnetate and intratumor injections of 5×10^9 plaque-forming units of recombinant Ad-eGFP-hNIS (*c*) or Ad-eGFP-rNIS solution (*b*) or sterile PBS (*a*). *1* thyroid gland, *2* transplanted tumor, *3* stomach. **B** Biodistribution of $^{99m}TcO_4^-$ in tumor-bearing rats. The NIS-expressing tumors exhibited an increased uptake of $^{99m}TcO_4^-$ compared with untransfected tumors. *hNIS* human sodium/iodide symporter; *rNIS* rat sodium/iodide symporter. $^*P < 0.05$ vs. control; $^{\#}P < 0.05$ vs. control

Furthermore, cells transfected with rNIS could uptake more radionuclide than hNIS. A number of previous studies showed that rNIS gene expression consistently yielded higher radioiodine uptake levels in every tested cell line, allowing using lower doses of ^{131}I for gene therapy [11, 20, 23]. However, there were some differences in the regulation mechanisms between the human and rat genes, as well as in the predicted hydrophilic and hydrophobic regions of the protein structure and in the orientation within the cellular membrane [11, 20, 23].

A time course assay was performed to study the uptake of radioiodine over time. Radioiodine uptake first increased and then reached a plateau. However, the efflux assay showed that ^{99m}Tc and ^{131}I were quickly secreted from the tumor cells, which was similar to a previous study showing that the elimination half-time was of about 15 min [24]. The main reason maybe is that iodine is not metabolized by non-thyroid cells.

^{99m}Tc emits gamma photons that can be used for imaging all organs and has been the most commonly used medical radionuclide since 1964 [s]. The present study showed that the xenograft tumors of bearing-tumor mice could be visualized through $^{99m}TcO_4^-$ uptake in the presence of the NIS gene. Biodistribution experiments showed the prominent intratumor uptake of $^{99m}TcO_4^-$ in hNIS mice compared with the rNIS group. Similarly, Chen et al. [26] injected hepatic carcinoma MH3924A cells into nude mice, and found that the hNIS tumor cells accumulated more $^{99m}TcO_4^-$ and that the xenografts yielded clear images.

Gene therapy represents the next era of medicine. The results of the present study are highly significant because they suggest that tumors could be modified in order to be targeted by an otherwise non-targeting imaging media/treatment. However, there are a large number of issues impairing the immediate applicability of these results. Indeed, in the present study, xenograft tumors were built from pure cells that were then transfected by intratumor virus injection. There are still issues with the specificity of viruses to the target cells, as well as the risk of viruses spreading to adjacent normal tissues. Many studies are needed before this approach could be implemented in whole animals or in human clinical trials. Nevertheless, these results are interesting and they suggest a promising new approach for imaging and treating cancer in general. Indeed, once the method is established using a lung cancer-specific vector, vectors targeting other cancer types could be easily established. However, some tissues constitutively express NIS (such as the thyroid and gastric tissues) and means to avoid radionuclide to go into these tissues should be explored before clinical trials. Promising experiments using telomerase-driven NIS expression could be a key to this problem [12, 27].

In conclusion, the rNIS and hNIS genes can be used as an effective method for the effective delivery of ^{99m}Tc and ^{131}I to specific tissues. Using the NIS genes, transfected A549/DDP human cisplatin-resistant lung cancer cells could effectively accumulate the ^{99m}Tc and ^{131}I and be noninvasively imaged using $^{99m}TcO_4^-$. Although much

more work is necessary before being able to cure cancer using gene therapy, the present study suggests that NIS expression in chemoresistant cancer cells can be used to detect cancer cells, and that the same system could be used to kill the cells using radionuclide. Future studies will look for a new tumor target, to visualize the tumor and to treat it using NIS.

Acknowledgments This work was supported by grants from the National Natural Sciences Foundation of China (81101068).

Conflict of interest Authors declare no conflict of interest or financial interests.

References

1. Jemal A, Bray F, Center MM, Ferlay J, Ward E, Forman D. Global cancer statistics. CA Cancer J Clin. 2011;61:69–90.
2. Herbst RS, Heymach JV, Lippman SM. Lung cancer. N Engl J Med. 2008;359:1367–80.
3. Wang QZ, Xu W, Habib N, Xu R. Potential uses of microRNA in lung cancer diagnosis, prognosis, and therapy. Curr Cancer Drug Targets. 2009;9:572–94.
4. Ma J, He X, Wang W, Huang Y, Chen L, Cong W, et al. E2F promoter-regulated oncolytic adenovirus with p16 gene induces cell apoptosis and exerts antitumor effect on gastric cancer. Dig Dis Sci. 2009;54:1425–31.
5. Wang X, Su C, Cao H, Li K, Chen J, Jiang L, et al. A novel triple-regulated oncolytic adenovirus carrying p53 gene exerts potent antitumor efficacy on common human solid cancers. Mol Cancer Ther. 2008;7:1598–603.
6. Chu CJ, Barker SE, Dick AD, Ali RR. Gene therapy for noninfectious uveitis. Ocul Immunol Inflamm. 2012;20:394–405.
7. Terrovitis J, Kwok KF, Lautamaki R, Engles JM, Barth AS, Kizana E, et al. Ectopic expression of the sodium-iodide symporter enables imaging of transplanted cardiac stem cells in vivo by single-photon emission computed tomography or positron emission tomography. J Am Coll Cardiol. 2008;52:1652–60.
8. Roelants V, Labar D, de Meester C, Havaux X, Tabilio A, Gambhir SS, et al. Comparison between adenoviral and retroviral vectors for the transduction of the thymidine kinase PET reporter gene in rat mesenchymal stem cells. J Nucl Med. 2008;49:1836–44.
9. Ahn BC. Sodium iodide symporter for nuclear molecular imaging and gene therapy: from bedside to bench and back. Theranostics. 2012;2:392–402.
10. Carrasco N. Iodide transport in the thyroid gland. Biochim Biophys Acta. 1993;1154:65–82.
11. Hu S, Cao W, Lan X, He Y, Lang J, Li C, et al. Comparison of rNIS and hNIS as reporter genes for noninvasive imaging of bone mesenchymal stem cells transplanted into infarcted rat myocardium. Mol Imaging. 2011;10:227–37.
12. Shi YZ, Zhang J, Liu ZL, Du SY, Shen YM. Adenovirus-mediated and tumor-specific transgene expression of the sodium-iodide symporter from the human telomerase reverse transcriptase promoter enhances killing of lung cancer cell line in vitro. Chin Med J (Engl). 2010;123:2070–6.
13. Ahn SJ, Jeon YH, Lee YJ, Lee YL, Lee SW, Ahn BC, et al. Enhanced anti-tumor effects of combined MDR1 RNA interference and human sodium/iodide symporter (NIS) radioiodine gene therapy using an adenoviral system in a colon cancer model. Cancer Gene Ther. 2010;17:492–500.
14. Jeon YH, Lee HW, Lee YL, Kim JE, Hwang MH, Jeong SY, et al. Combined E7-dendritic cell-based immunotherapy and human sodium/iodide symporter radioiodine gene therapy with monitoring of antitumor effects by bioluminescent imaging in a mouse model of uterine cervical cancer. Cancer Biother Radiopharm. 2011;26:671–9.
15. Lee YL, Lee YJ, Ahn SJ, Choi TH, Moon BS, Cheon GJ, et al. Combined radionuclide-chemotherapy and in vivo imaging of hepatocellular carcinoma cells after transfection of a triple-gene construct, NIS, HSV1-sr39tk, and EGFP. Cancer Lett. 2010;290:129–38.
16. Gunther M, Wagner E, Ogris M. Specific targets in tumor tissue for the delivery of therapeutic genes. Curr Med Chem Anticancer Agents. 2005;5:157–71.
17. Partlow KC, Chen J, Brant JA, Neubauer AM, Meyerrose TE, Creer MH, et al. 19F magnetic resonance imaging for stem/progenitor cell tracking with multiple unique perfluorocarbon nanobeacons. FASEB J. 2007;21:1647–54.
18. Dai G, Levy O, Carrasco N. Cloning and characterization of the thyroid iodide transporter. Nature. 1996;379:458–60.
19. Smanik PA, Liu Q, Furminger TL, Ryu K, Xing S, Mazzaferri EL, et al. Cloning of the human sodium iodide symporter. Biochem Biophys Res Commun. 1996;226:339–45.
20. Mitrofanova E, Unfer R, Vahanian N, Link C. Rat sodium iodide symporter allows using lower dose of 131I for cancer therapy. Gene Ther. 2006;13:1052–6.
21. Guo R, Zhang Y, Liang S, Xu H, Zhang M, Li B. Sodium butyrate enhances the expression of baculovirus-mediated sodium/iodide symporter gene in A549 lung adenocarcinoma cells. Nucl Med Commun. 2010;31:916–21.
22. Klutz K, Russ V, Willhauck MJ, Wunderlich N, Zach C, Gildehaus FJ, et al. Targeted radioiodine therapy of neuroblastoma tumors following systemic nonviral delivery of the sodium iodide symporter gene. Clin Cancer Res. 2009;15:6079–86.
23. Heltemes LM, Hagan CR, Mitrofanova EE, Panchal RG, Guo J, Link CJ. The rat sodium iodide symporter gene permits more effective radioisotope concentration than the human sodium iodide symporter gene in human and rodent cancer cells. Cancer Gene Ther. 2003;10:14–22.
24. Chen L, Altmann A, Mier W, Eskerski H, Leotta K, Guo L, et al. Radioiodine therapy of hepatoma using targeted transfer of the human sodium/iodide symporter gene. J Nucl Med. 2006;47:854–62.
25. Divgi CR. Status of radiolabeled monoclonal antibodies for diagnosis and therapy of cancer. Oncology. 1996;10:939–53.
26. Chen L, Altman A, Mier W, Lu H, Zhu R, Haberkorn U. 99mTc-pertechnetate uptake in hepatoma cells due to tissue-specific human sodium iodide symporter gene expression. Nucl Med Biol. 2006;33:575–80.
27. Riesco-Eizaguirre G, De la Vieja A, Rodriguez I, Miranda S, Martin-Duque P, Vassaux G, et al. Telomerase-driven expression of the sodium iodide symporter (NIS) for in vivo radioiodide treatment of cancer: a new broad-spectrum NIS-mediated antitumor approach. J Clin Endocrinol Metab. 2011;96:E1435–43.